Journal of Controlled Release 174 (2014) 27–36

Contents lists available at ScienceDirect

Journal of Controlled Release

journal homepage: www.elsevier.com/locate/jconrel

A novel cationic niosome formulation for gene delivery to the retina

G. Puras [a,b], M. Mashal [a], J. Zárate [a,b], M. Agirre [a,b], E. Ojeda [a,b], S. Grijalvo [b,c], R. Eritja [b,c], A. Diaz-Tahoces [b,d], G. Martínez Navarrete [b,d], M. Avilés-Trigueros [e], E. Fernández [b,d], J.L. Pedraz [a,b,*]

[a] NanoBioCel Group, University of the Basque Country, Vitoria-Gasteiz, Spain
[b] Networking Research Centre of Bioengineering, Biomaterials and Nanomedicine (CIBER-BBN), Zaragoza Spain
[c] Institute of Advanced Chemistry of Catalonia, IQAC-CSIC, Barcelona, Spain
[d] Neuroprothesis and Neuroengineering Research Group, Miguel Hernández University, Elche, Spain
[e] Laboratory of Experimental Ophthalmology, Faculty of Medicine, University of Murcia, Regional Campus of International Excellence "Campus Mare Nostrum", Murcia, Spain

ARTICLE INFO

Article history:
Received 29 July 2013
Accepted 4 November 2013
Available online 11 November 2013

Keywords:
Niosomes
Cationic lipids
Squalene
Non-ionic surfactant
Retina
Transfection

ABSTRACT

Niosomes represent a recent promising approach for gene delivery purposes. We elaborated on a novel niosome formulation based on the 2,3-di(tetradecyloxy)propan-1-amine cationic lipid, combined with squalene and polysorbate 80 to evaluate the transfection efficiency in rat retinas. Niosomes prepared by the solvent emulsification–evaporation technique were mixed with the pCMSEGFP plasmid to form lipoplexes which were characterized in terms of morphology, size, surface charge, and DNA condensation, protection and release. *In vitro* studies were conducted to evaluate transfection efficiency, viability and internalization mechanism in HEK-293 and ARPE-19 cells. The efficacy of the most promising formulation was evaluated in rat eyes by monitoring the expression of the EGFP after intravitreal and subretinal injections. Lipoplexes at 15/1 ratio were 200 nm in size, 25 mV in zeta potential and exhibited spherical morphology. At this ratio, niosomes condensed and protected the DNA from enzymatic digestion. Lipoplexes successfully transfected HEK-293 and specially ARPE-19 cells, without affecting the viability. Whereas lipoplexes entered mainly retinal cells by clathrin-mediated endocytosis, HEK-293 cells showed a higher caveolae-dependent entry. After ocular administration, the expression of EGFP was detected in different cells of the retina depending on the administration route. This novel niosome formulation represents a promising approach to deliver genetic material into the retina to treat inherited retinal diseases.

1. Introduction

Many devastating blinding disorders that affect the retina in the developed world have a well-known genetic background [1]. Despite the fact that gene therapy strategies have made major advances in recent years [2], many of the patients affected by inherited retinal diseases must live under impaired vision, even with the best medical treatment. Therefore, the development of effective gene carriers represents a major challenge for the scientific community [3]. At present, viral and non-viral vectors are the most employed approaches to deliver genetic material to the retina [4,5]. First promising clinical trial results with viral vectors in patients suffering from Leber's congenital amaurosis offered reasonable hope [6,7]. However, important concerns related to the risk of oncogenesis, immunogenicity, inflammatory responses, and the persistence of viral vectors in the brain after intravitreal injection [8] have garnered the interest to invest on non-viral gene transfer methods. Compared with their counterparts, non-viral vectors offer many important advantages, since they are less limited by the size of the gene to transfect, do not raise major safety concerns, are easier and cheaper to produce, and are classified as drugs rather than as biologist by the regulatory authorities. Among the challenges to face by non-viral vectors, the most important include transient gene expression duration and low transfection efficiency. However, tangible successes have been reported in retinal gene delivery application with some polymers [9,10], peptides [11] or liposomes [12,13]. Niosomes are non-ionic surfactant vesicles with a bilayer structure that have been widely applied in pharmaceutics since the 1980s as a demanding tool to improve the delivery of many drugs, such as chemotherapy drugs, peptides, antigens, hormones and other bioactive agents [14]. Basically, niosomes represent a drug delivery alternative to liposomes, in which phospholipids have been substituted by non-ionic surfactants. Compared with liposomes, niosomes are recognized for their low cost and superior chemical and storage stabilities. Nevertheless, few reports have focused on their application for gene delivery purposes [14], and according to our knowledge, there is no evidence related to the efficiency of niosomes as gene carriers for the retinal cells. In light of the excellent physicochemical properties for drug delivery, and the absence of literature reported on the use of niosome for gene delivery applications to the retina, we elaborated a novel cationic niosome formulation based on the 2,3-di(tetradecyloxy)propan-1-amine cationic lipid, combined with squalene and polysorbate 80. We hypothesized that this formulation

* Corresponding author at: Laboratory of Pharmacy and Pharmaceutical Technology, Faculty of Pharmacy, University of the Basque Country, 01006 Vitoria-Gasteiz, Spain. Tel.: +34 945013091; fax: +34 945013040.
E-mail address: joseluis.pedraz@ehu.es (J.L. Pedraz).

0168-3659/$ – see front matter © 2013 Elsevier B.V. All rights reserved.
http://dx.doi.org/10.1016/j.jconrel.2013.11.004

could function as a safe and effective non-viral vector for retinal gene delivery. Recently, it has been reported that the aforementioned cationic lipid was able to silence gene expression upon covalent conjugation with RNA molecules [15]; therefore, it could be an interesting positively charged lipid in the niosome formulation. Squalene is a natural lipid belonging to the terpenoid family that could be used instead of the classical cholesterol to enhance the rigidity and stability of the niosome formulation. Although it has been extensively used as excipient in pharmaceutical formulations for disease management and therapy, very few reports for gene delivery applications have been published [16]. Nevertheless, some authors have attributed flattering properties to squalene for gene therapy applications *in vitro* and *in vivo* with minimal cytotoxicity [17,18]. Polysorbate 80 is one of the most non-ionic surfactants employed in the niosome formulations that offers flattering properties for gene delivery purposes in terms of formulation and transfection efficiency, due to the presence of polyethylene glycol (PEG) chains in its structure [19,20]. To validate our speculations, we elaborated by the solvent emulsification-evaporation technique, cationic niosomes based on the 2,3-di(tetradecyloxy)propan-1-amine cationic lipid, in combination with different proportions of squalene and polysorbate 80. Particle size, polydispersity index (PDI) and zeta potential were measured, and the most promising formulation was used to form lipoplexes under gentle agitation with the pCMS-EGFP plasmid. Lipoplexes were elaborated at different cationic lipid/DNA ratios (w/w) and characterized by size, PDI, morphology, and the ability to condense and protect the DNA from enzymatic digestion. *In vitro* experiments were performed to evaluate the transfection efficiency, viability and internalization mechanism in HEK-293 and ARPE-19 cells. Following *in vitro* characterization, the best formulation was administered to rat eyes in order to evaluate the efficiency of the vectors to deliver genetic material into the retina after subretinal and intravitreal injections.

2. Materials and methods

2.1. Materials

HEK-293 cells, ARPE-19 cells, Eagle's Minimal Essential medium with Earle's BSS and 2 mM L-glutamine (EMEM) were obtained from the American Type Culture Collection (ATCC). Dulbecco's Modified Eagle's medium Han's Nutrient Mixture F-12 (1:1) was purchased from Gibco (San Diego, California, US). The plasmid pCMS-EGFP was purchased from PlasmidFactory (Bielefeld, Germany). The gel electrophoresis materials and gel red solution were acquired from Bio-Rad (Madrid, Spain). DNase I, sodium dodecyl sulfate (SDS), squalene, Nile Red and PBS were purchased from Sigma-Aldrich (Madrid, Spain), and dichloromethane was purchased from Panreac (Barcelona, Spain). AlexaFluor488-Cholera toxin and AlexaFluor488-Transferrin were provided by Molecular Probes (Barcelona, Spain), and Fluoromont G from SouthernBiotech (Coultek, Spain). Opti-MEM® reduced medium, antibiotic/antimicotic solution and Lipofectamine™ 2000 were acquired from Invitrogen (San Diego, California, US). Polysorbate 80 (Tween 80) was provided by Vencaser (Bilbao, Spain). The BD Viaprobe kit was obtained from BD Biosciences (Belgium).

2.2. Production of cationic niosomes

The cationic lipid was synthesized by modifying slightly the experimental protocol described previously [21]. Once the cationic lipid was synthesized, we elaborated the niosomes by the solvent emulsification–evaporation technique. Resulted cationic lipid was dissolved in 1 ml of the organic solvent dichloromethane (0.5%, w/v) containing squalene, and then emulsified in 5 ml of an aqueous phase with polysorbate 80. Different concentrations of squalene (v/v, in the organic phase) and polysorbate 80 (w/v, in the aqueous phase) were used. The emulsion was obtained by sonication (Branson Sonifier 250, Danbury) for 30 s at 50 W. The organic solvent was removed from the emulsion by evaporation under magnetic agitation for 4 h. Upon dichloromethane evaporation a dispersion containing the nanoparticles was formed by precipitation of the cationic nanoparticles in the aqueous medium.

2.3. Size, PDI and zeta potential measurements

The hydrodynamic diameter and the PDI were determined by dynamic light scattering (DLS), and the superficial charge by laser Doppler velocimetry (LDV) on a Zetasizer Nano ZS (Malvern Instruments, UK). Samples were diluted in NaCl 0.1 mM Milli-Q water, and the particle size, reported as hydrodynamic diameter, was obtained by cumulative analysis. All measurements were carried out in triplicate.

2.4. Preparation of cationic niosome/DNA lipoplexes

An appropriate volume of a pCMS-EGFP plasmid 0.5 mg/ml stock solution was added under gentle vortexing to different volumes of the cationic niosome suspension to get different cationic lipid/DNA ratios (w/w). Lipoplexes were incubated for 30 min at room temperature before use to enhance electrostatic interactions.

2.5. Morphology of cationic niosome/DNA lipoplexes

The morphology of the resulted lipoplexes was assessed by Transmission Electron Microscopy (TEM). Briefly, 5 μl of each sample was adhered onto glow discharged carbon coated grids for 60 s. Remaining liquid was removed by blotting on paper filter and stained with 2% uranyl acetate for 60 s. Samples were visualized under the microscope, Tecnai G2 20 Twin (FEI, Eindhoven, The Netherlands), operating at an accelerating voltage of 200 keV in a bright-field image mode. Digital images were acquired with an Olympus SIS Morada digital camera.

2.6. DNase I protection and SDS-induced release of DNA from lipoplexes

Naked DNA or lipoplexes samples (20 μl, containing 200 ng of the plasmid) were subjected to electrophoresis on an agarose gel (0.8%w/v) containing gel red staining. The gel was immersed in a Tris–acetate–EDTA buffer and exposed for 30 min to 120 V. Bands were observed under a digital, ChemiDoc MP Imaging System (Bio-Rad, Madrid, Spain). To analyze the release of DNA from the formulation, 20 μl of a 2% SDS solution was added to the samples. Protection capacity of the lipoplexes against enzymatic digestion was studied after adding DNase I (final concentration 1 U DNase I/2.5 μg DNA). Afterwards, the mixtures were incubated at 37 °C for 30 min. Finally, 2% SDS solution was added to release DNA from lipoplexes. The integrity of the DNA in each sample was compared with untreated DNA.

2.7. Cell culture and transfection protocol

HEK-293 and ARPE-19 cells were seeded in 24-well plates at an initial density of 15×10^4 and 7.5×10^4 cells/well, with 1 ml EMEM containing 10% horse serum and with 1 ml D-MEM/F-12 containing 10% fetal bovine serum, respectively. Then, at a confluence level of 70–80%, the media was removed and cells were exposed to different cationic lipid/DNA ratio (w/w) lipoplexes (1.25 μg DNA) diluted in serum-free Opti-MEM® solution for 4 h at 37 °C. Following the incubation time, the medium was refreshed with 1 ml of complete medium and cells were allowed to grow for further 72 h until fluorescence microscopy and flow cytometry analysis to determine transfection efficiency and cell viability [10]. Experiments with Lipofectamine™ 2000 (positive control) were prepared following the manufacturer's protocol.

Table 1
Composition and physicochemical characterization of niosome formulations. Mean (SD: standard deviation) (n = 3). The cationic lipid 2,3-di(tetradecyloxy)propan-1-amine was dissolved in the organic phase (0.5%, w/v) in all formulations. Lipoplexes characterization: Size, zeta potential and morphology.

Squalene (%, v/v)	Polysorbate 80 (%, w/v)	Size (nm)	Polydispersity index	Zeta potential (mV)
1	1	151.33 ± 4.41	0.565 ± 0.06	42.46 ± 2.23
1	0.5	280.61 ± 6.53	0.656 ± 0.02	53.60 ± 6.33
2	1	161.70 ± 0.43	0.321 ± 0.02	51.26 ± 4.18
2	0.5	257.83 ± 0.70	0.230 ± 0.01	53.53 ± 0.83

2.8. Internalization mechanism

The endocytosis mechanisms were evaluated qualitatively by colocalization studies with Nile Red-labeled lipoplexes and AlexaFluor488-Cholera Toxin (10 μg/ml) or AlexaFluor488-Transferrin (50 μg/ml), which are markers of caveolae raft-mediated endocytosis and clathrin-mediated endocytosis, respectively. To elaborate on Nile Red-labeled niosomes, the Nile Red dye (0.25%, w/v) incorporated into the dichloromethane phase employed to prepare the niosomes by the previously described emulsification–evaporation technique. Briefly, cells at the appropriate density were seeded in 24-well coverslips containing plates and co-incubated with Nile Red-labeled lipoplexes and either AlexaFluor488-Cholera Toxin or AlexaFluor488-Transferrin for 2 h. Next, the medium containing lipoplexes was removed and cells were washed twice with PBS, fixed with a 4% paraformaldehyde solution and nuclei were labeled with Hoechst 33342. Preparations were mounted on Fluormount G and visualized with an Olympus Fluoview 500 confocal microscopy under sequential acquisition to avoid overlap of fluorescent emission spectra.

2.9. In vivo studies in rats

Adult male Sprague–Dawley rats (6–7 weeks old, 150–200 g weight) were used as experimental animals. All experimental procedures were carried out in accordance with the Spanish and European Union regulations for the use of animals in research and the Association for Research in Vision and Ophthalmology (ARVO) statement for the use of animals in ophthalmic and vision research and supervised by the Miguel Hernandez University Standing Committee for Animal Use in Laboratory. The surgical procedures used for the administration of the vectors in the retina have been described elsewhere [9,10].

2.10. Intravitreal and subretinal injections

The animals (n = 3) received through intravitreal or subretinal route a 4 μl suspension based on cationic niosomes/DNA lipoplexes containing 100 ng of the plasmid. Injections were performed under an operating microscope (Zeiss OPMI® pico; Carl Zeiss Meditec GmbH, Jena, Germany) with the aid of a Hamilton microsyringe (Hamilton Co., Reno, NV). A bent 34-gauge needle was used to inject into the vitreous of the left eye, immediately adjacent to the ora serrata without touching the lens. To deliver the lipoplexes into the subretinal space the needle was passed through the sclerotomy 2 mm posterior to ora serrata and in a tangential direction toward the posterior retinal pole along the subretinal space. Successful administration was confirmed by the appearance of a partial retinal detachment by direct ophthalmoscopy of the eye fundus. The untreated right eye served as a control. Three days post-injection, the rats were sacrificed and perfused with 0.9% saline followed by 4% paraformaldehyde in 0.1 M phosphate buffer (pH 7.2–7.4) at 4 °C.

2.11. EGFP immunostaining

Protein expression was evaluated in sagittal sections of the retina. Briefly, both eyes were enucleated, and the anterior segments, including the lens, were removed. Posterior eyecups were fixed as described above. Samples were then immersed in a graded series of sucrose solutions, 15%, 20% and 30% in PBS overnight at 4 °C for cryoprotection. Eyecups were embedded and oriented in optimal cutting temperature (O.C.T.™) compound (Tissue-Tek®; Sakura Finetek Europe B.V., Alphen and den Rijn, The Netherlands) and frozen in 2-methylbutane cooled in liquid nitrogen at −60 °C. Radial sections (16 μm) were cut with a cryostat (HM 550; Microm International GmbH, Walldorf, Germany), mounted on SuperFrost® Plus microscope slides (VWR International BVBA, Leuven, Belgium). Prior to immunostaining, the frozen sections were blocked through non-specific staining with 10% normal donkey serum for 1 h with 0.5% Triton X-100 and then incubated overnight at room temperature with combinations of the primary antibodies: Chicken anti-GFP (Invitrogen), mouse anti-PKC (Santa Cruz Biotechnology), rabbit anti-NeuN (Millipore), goat anti-Vimentin (Santa Cruz Biotechnology), and rabbit anti-Parvalbumin (Calbiochem). The primary antibody was visualized using Alexa Fluor 488, Alexa Fluor 555, and Alexa Fluor 633-conjugated secondary antibodies (Molecular Probes). Immunofluorescence and EGFP expression were evaluated using a Leica TCS SPE spectral confocal microscope (Leica Microsystems GmbH, Wetzlar, Germany). Images were processed, montaged and composed digitally using ImageJ (National Institutes of Health, Bethesda, MD) and Adobe® Photoshop® CS5.1 (Adobe Systems Inc., San Jose, CA) software.

2.12. Statistical analysis

Statistical analysis was completed with the InStat program (GraphPad Software, San Diego, CA, USA). Differences between groups at significance levels of 95% were calculated by the Student's *t* test. In all cases, P values < 0.05 were regarded as significant. Normal

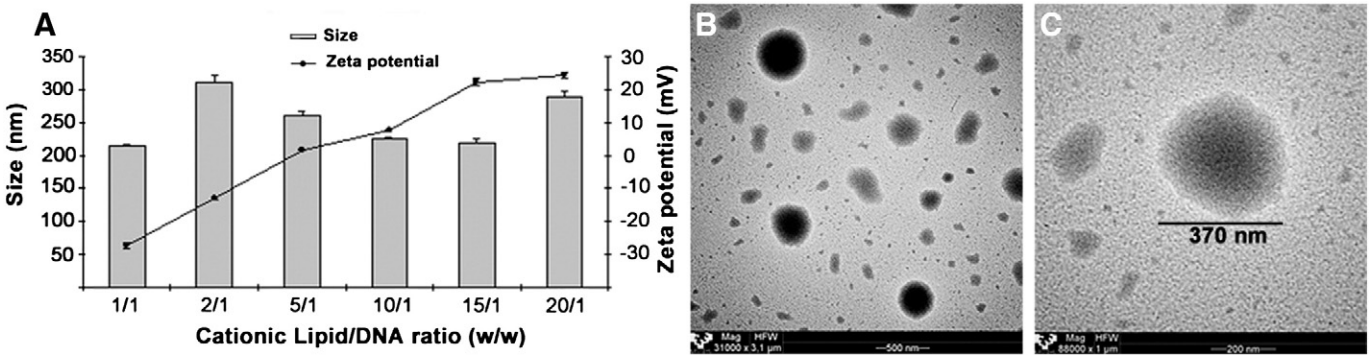

Fig. 1. Lipoplexes characterization. A) Effect of cationic lipid/DNA ratio (w/w) on zeta potential and size (mean ± SD, n = 3). B, C and D) TEM images of lipoplexes at 15/1 charge ratio, original magnification 31.000× and 88.000× respectively.

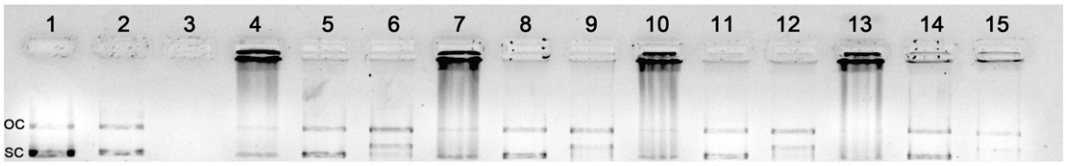

Fig. 2. Binding, protection, and SDS-induced release of DNA from niosomes at different cationic lipid/DNA ratios (w/w) visualized by agarose electrophoresis. Lanes 1–3 correspond to free DNA; lanes 4–6, cationic lipid/DNA 5/1; lanes 7–9, cationic lipid/DNA 10/1; lanes 10–12, cationic lipid/DNA 15/1; lanes 13–15, cationic lipid/DNA 20/1. Lipoplexes were treated with SDS (lanes 2, 5, 8, 11 and 14) and DNase I + SDS (lanes 3, 6, 9, and 15). OC: open circular form, SC: supercoiled form.

distribution of samples was assessed by the Kolmogorov–Smirnov test, and the homogeneity of the variance by the Levene test. Data were presented as mean ± SD, unless stated otherwise.

3. Results

3.1. Composition and physicochemical characterization of cationic niosomes

Table 1 summarizes particle size, PDI and zeta potential of niosomes composed of cationic lipid 2,3-di(tetradecyloxy)propan-1-amine (0.5%, w/v), combined with different amounts of squalene and polysorbate 80. All formulation varied in size, PDI and zeta potential depending on the percentage of squalene and polysorbate 80. Squalene percentage in the formulation did not affect particle size as much as polysorbate 80. Niosome size only varied from 280 to 257 nm at low polysorbate 80 percentages, and from 151 to 161 nm at high polysorbate 80 percentages, whereas size clearly decreased from 280 to 151 nm and from 257 to 161 at low and high polysorbate 80 percentages, respectively. Regarding PDI, a clear decrease from 0.65 to 0.23, and from 0.56 to 0.32 was observed when squalene percentage in the formulation increased at both low and high levels of polysorbate 80 respectively, whereas only a slight decrease in the PDI value from 0.65 to 0.56 and from 0.32 to 0.23 was observed when polysorbate 80 percentage increased at low and high values of squalene. The effect of squalene on zeta potential depended on the polysorbate 80 percentage. At low polysorbate 80

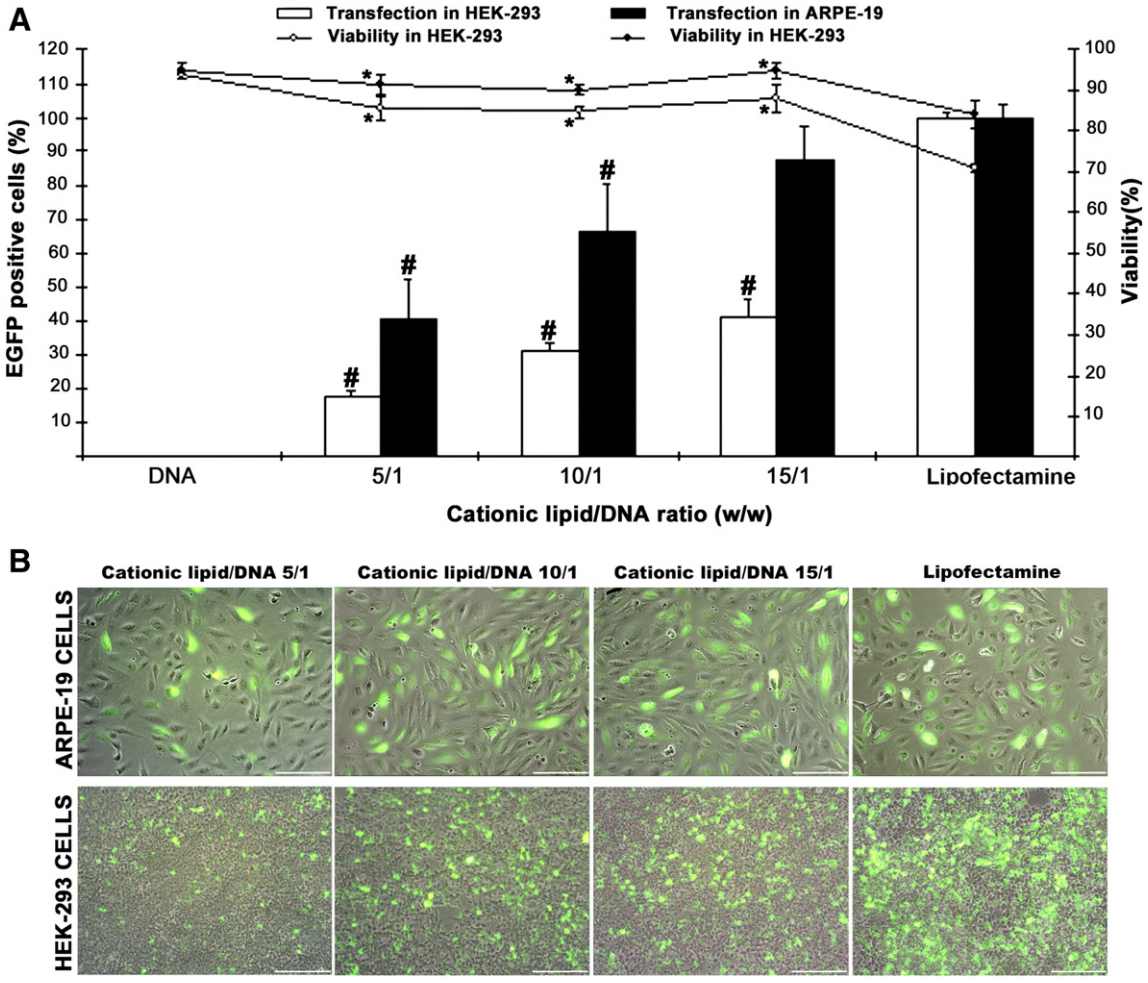

Fig. 3. Transfection efficiency and cell viability of lipoplexes in ARPE-19 and HEK-293 culture cells at 72 h-post transfection. A) Evaluation by flow cytometry of the percentage of EGFP positive cells (bars) and the viability (lines) at different cationic lipid/DNA ratios (w/w). Transfection percentages were normalized to Lipofectamine™ 2000. Values represent mean ± SD, n = 3 ($^{\#}P < 0.05$ relative to Lipofectamine™ transfection) ($^{*}P < 0.05$ relative to Lipofectamine™ viability). B) Overlay phase-contrast micrographs with fluorescent illumination (GFP channel) of ARPE-19 and HEK-293 cells transfected with niosomes at different cationic lipid/DNA ratios (w/w) and with Lipofectamine™ 2000. Scale bar = 100 μm.

percentages, zeta potential remains constant at 53 mV, whereas at high polysorbate 80 percentages, zeta potential increases from 42 to 51 mV when squalene percentage in the formulation increases.

Cationic niosome–DNA lipoplexes were prepared with niosomes composed of 2,3-di(tetradecyloxy)propan-1-amine cationic lipid, combined with 2% of squalene and 0.5% of polysorbate 80. As can be observed form Fig. 1A, size and zeta potential values of lipoplexes were affected by the cationic lipid/DNA ratio (w/w). Particle size ranged from 215 nm at 1/1 ratio to 310 nm at 2/1 ratio. In all cases, PDI was below 0.3 (data not shown). Regarding zeta potential, negative values were obtained at 1/1 and 2/1 ratios (−27 and −12 mV respectively). The first positive zeta potential value, 1.6, was reached at 5/1 ratio and it increased gradually with the mass ratio until a maximum value of 24 mV, at 20/1 ratio. The morphology of lipoplexes at 15/1 ratio was assessed by TEM as illustrated in Fig. 1B and C (original magnification 31.000× and 88.000× respectively). Under our experimental conditions cationic niosome/DNA lipoplexes exhibited a discrete spherical morphology.

3.2. Binding, DNaseI protection and SDS-induced release of DNA

Fig. 2 shows the results obtained in the agarose gel electrophoresis assay. All cationic lipid/DNA ratios were able to bind the DNA, since intensive bands were observed on wells 4, 7, 10 and 13 which

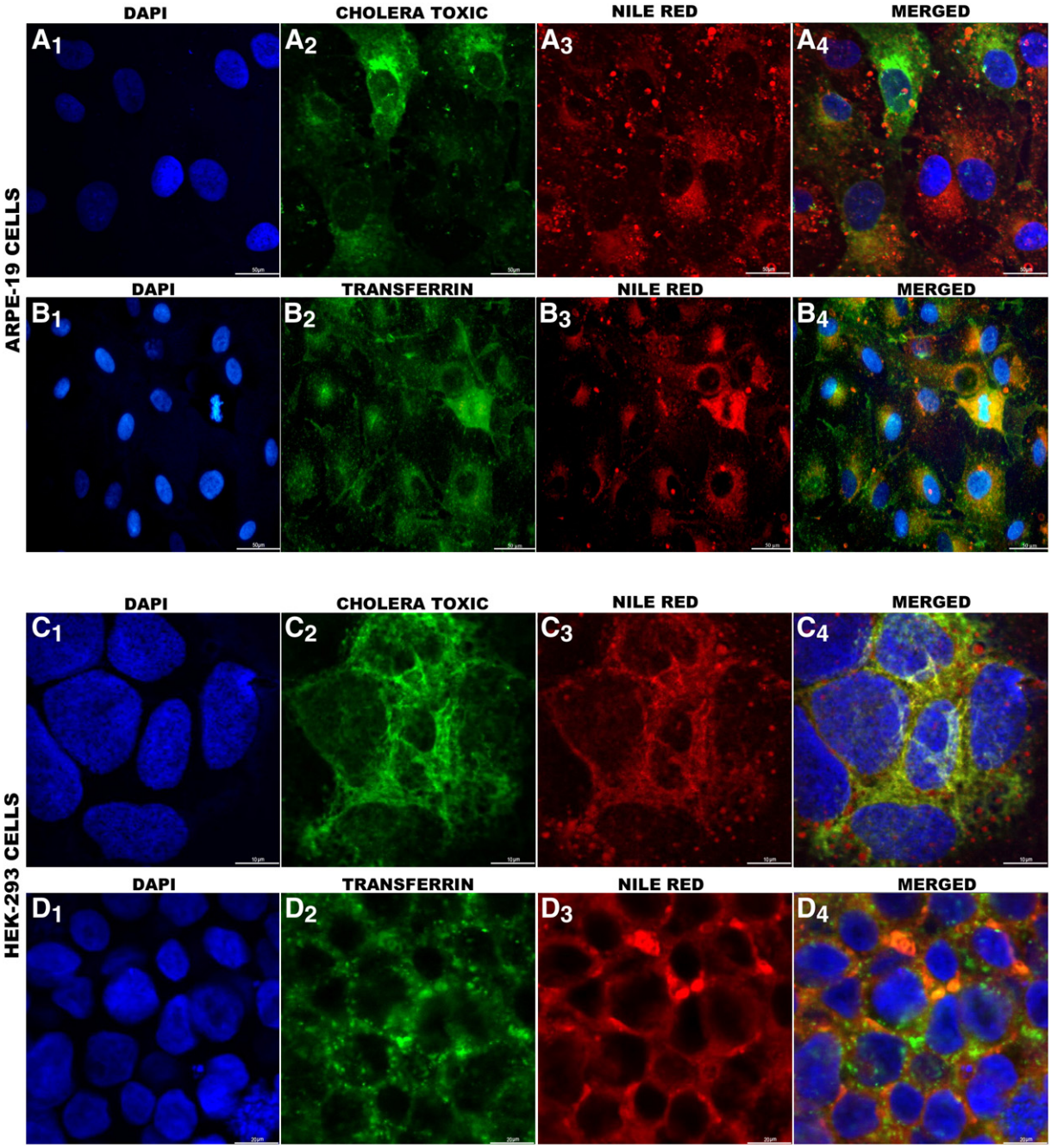

Fig. 4. Confocal microscopy images showing the intracellular distribution of ARPE-19 and HEK-293 cells. Each image shown on the optical section was representative of the cell population. Blue coloring shows cell nuclei stained with Hoechst 33258 (A_1, B_1, C_1 and D_1), green coloring shows cells stained with AlexaFluor488-Cholera toxin (A_2, C_2) or AlexaFluor488-Transferrin (B_2, C_2), and red coloring shows cells incubated with Nile Red-labeled niosome–DNA lipoplexes (A_3, B_3, C_3 and D_3). Merged images show cells coincubated with Nile Red-labeled niosome–DNA vectors, Hoechst 33342 and AlexaFluor488-Cholera toxin (A_4, C_4) or AlexaFluor488-Transferrin (B_4, C_4).

corresponded to 5/1, 10/1, 15/1 and 20/1 ratios respectively. Upon the addition of SDS, the DNA was successfully released from all formulations, since clear SC (supercoiled) bands were observed on lanes 5, 8, 11 and 14 (5/1, 10/1, 15/1 and 20/1 ratios). SC bands on lanes 6, 9 and 12 revealed that the DNA was protected from enzymatic digestion and released after the addition of SDS at 5/1, 10/1 and 15/1 ratios. However, at 20/1 ratio (lane 15), part of the DNA remained on the well and was not successfully released from the formulation after the treatment with SDS. No band on lane 3 suggested that free DNA was completely digested by the enzyme.

3.3. Transfection efficiency and viability in HEK-293 and ARPE-19 culture cells

Fig. 3 represents the transfection efficiency and viability of cationic niosome/DNA lipoplexes in ARPE-19 and HEK-293 culture cells. As observed on Fig. 3A, the number of transected cells increased gradually with the mass ratio, both in HEK-293 (white bars) and in ARPE-19 cells (black bars). At all ratios tested, the percentage of transfection was higher in ARPE-19 cells, which ranged from 40% at 5/1 ratio to a maximum of 88% at 15/1 ratio (data normalized to Lipofectamine™ 2000, 57% of absolute transfection). At this point, we did not find statistical differences in transfection efficiency when compared with Lipofectamine™ 2000. The percentages of transfection in HEK-293 ranged from 18% to 41% at 5/1 and 15/1 ratios respectively (data normalized to Lipofectamine™ 2000, 68% of absolute transfection). Free DNA did not transfect neither HEK-293 nor ARPE-19 cells. Regarding cell viability, Lipofectamine™ 2000 was significantly more toxic ($P < 0.05$) to HEK-293 (70% viability) and ARPE-19 (84% viability) cells than the cationic niosome/DNA lipoplexes at all ratios tested (Fig. 3A, lines). In ARPE-19 cells, viability was always over 90%, whereas viability in HEK-293 cells ranged from 84 to 87% at all ratios tested. Fig. 3B shows pictures of ARPE-19 and HEK-293 cells transfected with cationic niosome/DNA lipoplexes at different ratios. Under microscopic examination, ARPE-19 and HEK-293 cells revealed a healthy morphology at all formulations tested.

3.4. Internalization mechanism of Nile Red-labeled lipoplexes

Internalization mechanism in ARPE-19 and HEK-293 cells was studied by CLSM (Fig. 4). In HEK-293 cells, colocalization of Nile Red lipoplexes with cholera toxin was higher than with transferrin (merged pictures in HEK-293 cells); however, in ARPE-19 cells, colocalization of Nile Red niosomes with transferrin was higher than with cholera toxin (merged pictures in ARPE-19 cells). These findings indicate that in ARPE-19 cells, lipoplexes mainly entered by clathrin-mediated endocytosis, whereas HEK-293 cells showed a higher caveolae-dependent entry.

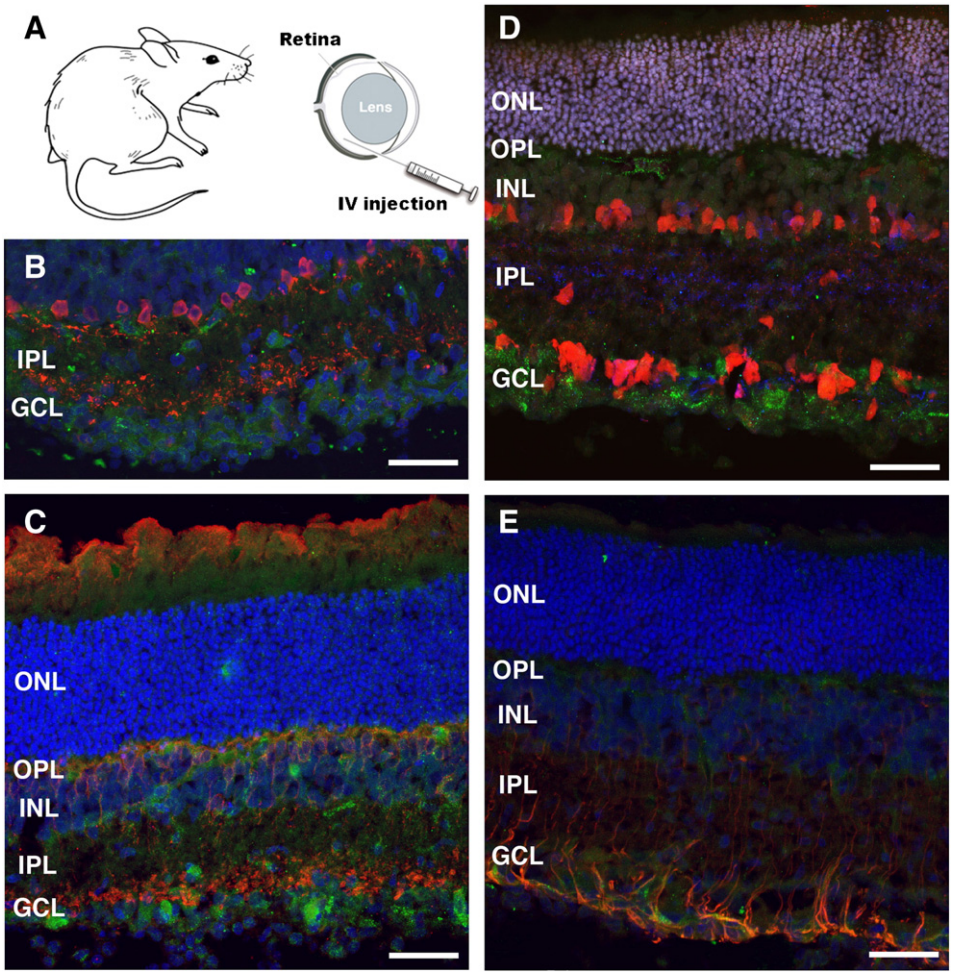

Fig. 5. *In vivo* gene expression of EGFP after intravitreal injection of niosome–DNA lipoplexes at 15/1 cationic lipid/DNA ratio. (A) Schematic drawing of the intravitreal injection. (B, C, D, E) Distribution of EGFP-positive cells and partial double-staining colocalization of EGFP. Images show the GFP expression with Parvalbumin in the INL (B), with bipolar cell marker protein kinase C (PKC) (C), with NeuN-positive ganglion cells in the GCL (D) and with Vimentin Müller cell markers (E). Cell nuclei were counterstained with Hoechst 33342 (pseudocolored blue). ONL (Outer nuclear layer), OPL (Outer plexiform layer), INL (Inner nuclear layer), IPL (Inner plexiform layer), GCL (Ganglion cell layer). Scale bars = 40 μm.

3.5. In vivo transfection experiments

Significant EGFP expression was detected only in the eyes treated with cationic niosome–DNA lipoplexes at 15/1 cationic lipid/DNA ratio after both intravitreal and subretinal administrations (Figs. 5A, 6A). No gene expression was detected after administration of the DNA solution (data not shown). The level of protein expression varied depending on the location of the injection. Thus, after intravitreal injection (Fig. 5), EGFP expression was found mainly at the ganglion cell layer (GCL), inner plexiform layer (IPL) and inner nuclear layer (INL). Some EGFP-positive neurons in the INL are labeled for Parvalbumin (Fig. 5B) whereas other EGFP cells co-label with PKC-positive bipolar cells (Fig. 5C). We also found NeuN-positive cells that were EGFP-positive in the ganglion cell layer (GCL) (Fig. 5D). Double labeling with Vimentin, a Müller glial cell marker, indicates that many of the EGFP-positive cells express this glial marker (Fig. 5E).

Similar results were obtained for subretinal injections (Fig. 6) although in this case EGFP expression was also found in the retinal pigment epithelium layer (RPE, Fig. 6B). Likewise we observed EGFP expression in the GCL (Fig. 6C) and there were also EGFP cells in the INL. Furthermore we also found partial colocalization of EGFP with the bipolar cell marker PKC (Fig. 6D) and with Vimentin (Fig. 6E).

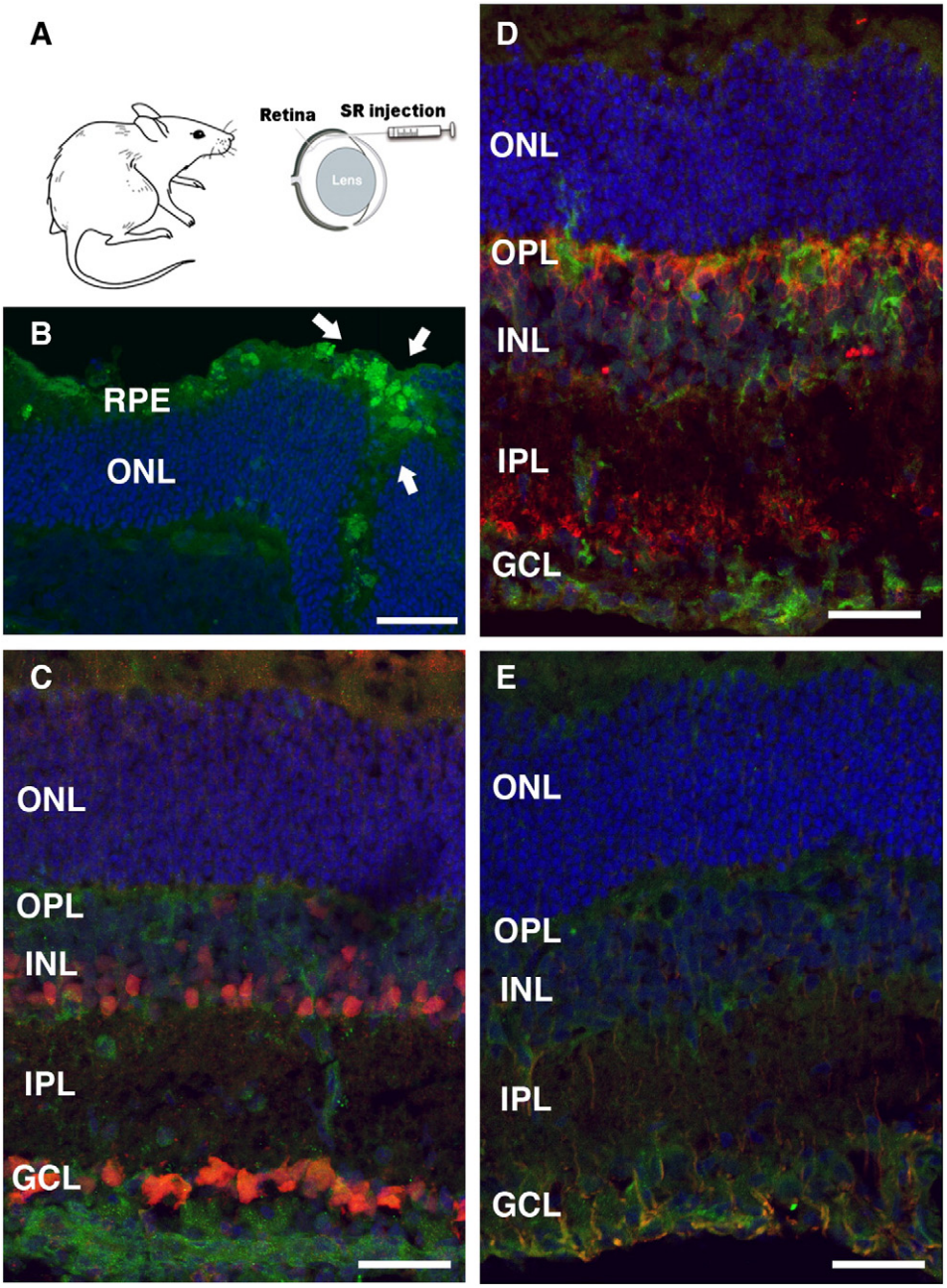

Fig. 6. *In vivo* gene expression of EGFP after subretinal injection of niosome–DNA lipoplexes at 15/1 cationic lipid/DNA ratio. (A) Schematic drawing of the subretinal injection. (B) Confocal fluorescence micrographs of retinal cross sections showing intense labeling in RPE cells (arrows). (C, D, E) Most EGFP-positive cells were located in the INL and GCL. Double labeling of EGFP shows some partial coexpression with NeuN (C), PKC (D) and Vimentin (E) in the retina. Cell nuclei were counterstained with Hoechst 33342 (pseudocolored blue). RPE (Retinal pigment epithelium), ONL (Outer nuclear layer), OPL (Outer plexiform layer), INL (Inner nuclear layer), IPL (Inner plexiform layer), GCL (Ganglion cell layer). Scale bars = 40 μm.

4. Discussion

Despite the fact that viral vectors have been widely used as gene carriers for inherited retinopathies [5], relevant safety concerns have garnered the interest of the scientific community to invest on non-viral gene transfer strategies. However, additional work, including the synthesis of new vectors, is required to improve their transfection efficiency and viability. Therefore, we elaborated a novel non-viral vector based on the 2,3-di(tetradecyloxy)propan-1-amine cationic lipid, squalene and polysorbate 80 for gene delivery to the retina.

The chemical structure of the 2,3-di(tetradecyloxy)propan-1-amine cationic lipid (see Supplementary data) offers hope for gene delivery applications [15], since it contains four domains (polar head, non-polar hydrophobic chains, linker and backbone) that rule the transfection processes. However, the ether bond of the linker domain is more toxic to the cells than the counterpart ester bond [22]. To circumvent this problem, we combined the non ionic surfactant polysorbate 80 with the cationic lipid to form niosomes, since it has been reported that the presence of polysorbate 80 decreases the proportion of the cationic lipid in the formulation, which enhances the tolerance of the cells [23]. In addition, polysorbate 80 acts as an emulsifier creating a steric barrier that avoids aggregation [19], and the presence of polyethylene glycol (PEG) chains in its structure improves transfection efficiency of liposome formulations [20]. Therefore, polysorbate 80 shows flattering properties for gene therapy in terms of formulation and transfection efficiency. In order to enhance the stability and rigidity of the vesicles, we incorporated squalene into the niosome formulation, instead of the classical cholesterol. Squalene, a natural lipid belonging to the terpenoid family, is a biochemical precursor of cholesterol and other steroids. Unlike cholesterol, squalene lacks a hydroxyl group. Therefore, we hypothesize that squalene is located in the hydrophobic core of the niosome bilayer. Although squalene has been extensively used as excipient in pharmaceutical formulations for disease management and therapy, very few reports in gene delivery have been published [17].

Since gene transfection mediated by cationic niosomes can be affected by the concentration of its components, we analyzed the effect of squalene and polysorbate 80 on the size, PDI and zeta potential of niosomes. As summarized in Table 1, polysorbate 80 clearly decreased the particle size, probably due to its intrinsic viscosity [24], while squalene clearly affected the PDI. Squalene has a high interfacial tension against water, which could explain the decrease of the PDI values observed when used at high concentrations. Regarding zeta potential, values decreased when the niosomes were formulated at low percentages of squalene and high polysorbate 80 percentages, probably due to neutral PEG chains of the polysorbate 80 in the bilayer surface. According to the results obtained on Fig. 1, we elaborated on cationic niosomes based on the 2,3-di(tetradecyloxy)propan-1-amine cationic lipid (0.5% w/v) polysorbate 80 (0.5%, w/v) and squalene (2%, w/v), obtaining particles of appropriate size for gene therapy purposes, 257 nm, with low PDI, 0.23, and high zeta potential, 53 mV, to interact electrostatically whit the negatively charged phosphate groups of the DNA (Table 1). Once the niosome formulation was characterized in terms of size, PDI and zeta potential, we formulated lipoplexes with the pCMS-EGFP plasmid varying the mass ratio between the cationic lipid and the DNA (w/w ratio).

Lipoplexes characterization data are represented on Fig. 1. It has been widely reported that uptake and transfection efficiency of lipoplexes strongly depend on the size of the vectors. Although there is not a general rule about the optimum particle size of lipoplexes for gene therapy, it is generally accepted that the mass ratio affects the particle size. In our experimental conditions, particle sizes ranged from 215 nm at 1/1 ratio to 310 nm at 2/1 ratio (Fig. 1A, bars). This increment in the particle size can be explained by the greater space demanded by the lipid in the formulation; however, as the proportion of the lipid increases, the DNA is more condensed in the formulation, due to the electrostatic interactions, which could explain the minimal oscillations observed in the particle size at the rest of the ratio tested. Therefore, particle size can depend on a delicate balance between the ability of the cationic lipid to precondense the DNA and the greater space demanded by itself. Regarding zeta potential, we found a clear relationship between the cationic lipid/DNA ratio and the superficial charge (Fig. 1A, lines). The positive correlation demonstrates that the cationic niosomes were able to bind and neutralize the negative charges of the DNA [25]. Therefore, lipoplexes at ratios above 5/1 may be able to function as carriers in gene therapy, since it has been widely postulated that the positively charged lipoplexes can interact electrostatically with the negatively charged cell surface, inducing early steps of the endocytosis process [26]. To get a direct evidence of the lipoplexes formation, we examined lipoplexes at 15/1 mass ratio under a TEM microscope at different magnifications. According to the pictures (Fig. 1C), particle size was around 370 nm, slightly bigger than the reported by dynamic light scattering (220 nm, Fig. 1A, bars). Such differences in the size of the particles could be explained by the sample manipulation required to perform TEM analysis. The well-defined vesicle shapes observed exhibited discrete spherical morphology, indicating that the strategy of substituting cholesterol with squalene worked reasonably well, presumably due to the similar parent structure.

The optimal conditions for complex formation were determined using a gel retardation assay at mass ratios ranging from 5/1 to 20/1 (Fig. 2). The 1/1 and 2/1 ratios were discharged because of the negative zeta potential (Fig. 1A, lines). The rest of the ratios were able to complex and release the DNA, upon the addition of SDS. Regarding the protection against enzymatic digestion, SC bands observed on lanes 6, 9 and 12 indicate that the DNA was protected from enzymatic digestion at 5/1, 10/1 and 15/1 ratios respectively. However, at 20/1 ratio, we did not observe a clear SC band on lane 15, because part of the DNA was retained in the well and it was not released from the niosomes upon the addition of SDS, probably due to the high electrostatic interaction between the cationic lipid and the DNA. Therefore, we did not check charge ratios over 30, since an optimum balance between DNA complexation and release from lipoplexes is required for an efficient transfection [25]. Once we evaluated that our formulations were biotechnologically suitable for gene therapy purposes, we studied *in vitro* the transfection efficiency and cell viability of cationic niosome/DNA lipoplexes at 5/1, 10/1 and 15/1 ratios in a well known model for transfection studies such as the HEK-293 cells, and in a cell line of the retina more difficult to be transfected such as the ARPE-19, which plays a major role in retinal diseases associated with senescence and dystrophies of the photoreceptors [27]. The 20/1 ratio was discharged for the *in vitro* transfection studies due to the difficulties observed by this formulation to release the DNA (Fig. 2, lane 15). Data are summarized on Fig. 3. Transfection efficiency in both cell lines was evaluated at 72 h, since we have observed that at this time, both cell lines reached the maximum peak of transfection (data not shown). Transfection efficiency in HEK-293 and ARPE-19 cells increased in proportion to the ratio, reaching the maximum at 15/1. At this point, there were no significant differences in transfection efficiency between ARPE-19 cells treated with niosomes and with Lipofectamine™ 2000 (Fig. 3A, bars). Additionally, at all ratios tested, transfection in ARPE-19 cells was higher than in HEK-293. These promising data reveal the suitability of this formulation to transfect efficiently retinal cells. Therefore, it could be an interesting alternative to Lipofectamine, since some authors have reported damage on the retina associated to the in vivo administration of Lipofectamine in the eye [28]. However, not always may exits in vitro–in vivo correlation, mainly due to physical barriers [29]. Therefore, aditional in vivo studies are required to comfirm in vitro results. Regarding toxicity (commonly associated with the induction of apoptosis), cationic lipid/DNA lipoplexes were well tolerated by the cells at all ratios tested, resulting in viability percentages higher than Lipofectamine™ 2000 both in ARPE-19 and HEK-293 cells (Fig. 3, lines). Interestingly, viability in ARPE-19 was superior when compared to HEK-293 cells at all ratios tested. Therefore our *in vitro* results reveal that lipoplexes transfected efficiently ARPE-

19 cells, without compromising the viability of the cells at the doses evaluated. Based on the *in vitro* transfection results, we decided to study the cellular uptake of the lipoplexes in order to explain the differences observed in the transfection efficiency between both cell lines, since this process is highly cell-dependent and clearly affects the transfection efficiency [30]. However, we found that lipoplexes entered efficiently in both cell lines since the first hour in contact with the formulations (data not shown). Probably, the high zeta potential value of the lipoplexes (22.5 mV) and the lipophilicity of the formulation contributed to the efficient uptake. Considering these results, we hypothesized that transfection differences observed between both cell lines could not be attributed to differences into the cellular uptake efficiency, but to the internalization mechanism.

Since transfection efficiency is highly determined by the endocytosis mechanism [31], which is highly cell line dependent, we performed CLSM studies in both cell lines with Nile Red-labeled cationic niosome/DNA lipoplexes and markers for two of the most employed pathways involved in the endocytosis processes of lipoplexes, such as the caveolae and the clathrin-mediated endocytosis [32]. Results are presented in Fig. 4. According to CLSM images, lipoplexes mainly colocalized with transferrin marker in ARPE-19 cells, whereas in HEK-293 cells, colocalization was mainly observed with cholera-toxin. These finding suggest that clathrin-mediated endocytosis is the main entry mechanism in ARPE-19 cells, whereas in HEK-293 cells, lipoplexes entered as observed in gene expression between both cell lines. However, other endocytosis mechanisms such as phagocytosis, macropinocytosis or clathrin/caveolae-independent endocytosis could be involved in the entry of the lipoplexes [31].

It is generally accepted that caveolae uptake is advantageous over clathrin in terms of DNA delivery, since it avoids lysosomal degradation [33]. However, formulations that enter *via* caveolae need to escape from caveosome in order to transfect efficiently. Likewise, the lack of lysosomal activity in the caveosome could hamper the release of the DNA from the niosome formulation, which could explain, in part, the low transfection efficiency observed in HEK-293 cells [34]. Regarding the clathrin-mediated pathway, one of the best characterized types of endocytosis [35], it has been described as the main pathway for cationic lipid-based systems [36]. Genes that are internalized through clathrin-mediated endocytosis are usually trapped in endosomes, which fuse with lysosomes resulting in a degradation of the content [37]. Therefore, a timely release of the DNA from the endosome is necessary in this pathway to get efficient gene expression [38]. The incorporation of co-lipids such as DOPE or cholesterol in lipidic formulation enhances the endosomal escape, and therefore the gene expression. Upon certain circumstances these helper lipids promote L_{α}–H_{II} transition (lamellar to inverse hexagonal phase transition), which enhances the release of nucleic acids across endosomes into the cytoplasm, resulting in high transfection efficiencies [39]. Interestingly, it has been recently shown that coupling squalene to gemcitabine results in nanoassemblies with inverse hexagonal structure [40]. Therefore, we hypothesize that squalene (a precursor of the cholesterol synthesis) could enhance endosomal escape of the plasmid, resulting in high levels of gene expression in ARPE-19 cells. Additional cryo-TEM or small-angle X-ray scattering (SAXS) studies would be required to determine the supramolecular structures of our lipoplexes, in order to validate our hypothesis. Since the internalization mechanism is highly dependent on the composition of the formulations, knowledge on this topic can be helpful to design more efficient non-viral vectors for gene therapy purposes.

We carried out a further preliminary *in vivo* study based on the low toxicity and the high percentage of ARPE-19 cells transfected with the niosome formulation to assess whether the vectors were able to transfect the rat retinas after intravitreal (Fig. 5) and subretinal injections (Fig. 6). These routes are the most effective ways to deliver material to the posterior segment of the eye, and are clinically viable options [41]. Our results show that both routes were successful to target cells at the GCL and INL. In addition, the subretinal injection was also able to transfect RPE cells. Mutations in genes specific to photoreceptors or RPE cells can result in many inherited retinal diseases [2]. To date, mutations in over 200 genes have been associated with genetic disorders of the retina such as retinitis pigmentosa or Leber congenital amaurosis (http://www.sph.uth.tmc.edu/RetNet). Therefore, transfection at this level of the retina is highly desirable for therapeutic purposes [42]. However, possible complications related with this route, such as retinal detachment, often dissuade its clinical application. Likewise, the effect of subretinal injection is generally localized around the injection site, although we found pretty diffusion to the inner layers of the retina (Fig. 6C, D and E). By contrast, intravitreal injection is a safer technique and is more widely used in the clinical practice. Generally, intravitreal injections deliver the genetic material to a larger retinal surface [43]. We found a good and uniformly distributed response in the inner layers of the retina when intravitreal injection was employed (Fig. 5), which suggests a partial diffusion of the lipoplexes through the inner layer of the retina; enhanced probably, by the ability of the PEG chains of the polysorbate 80 structure to prevent aggregations due to interaction with fibrillar structures in the vitreous [29]. However, we did not target the outer retina by intravitreal injections, which is one of the greatest challenges demanded for non-viral vectors. Transfection at the inner layers of the retina could be interesting to treat some genetic pathologies of the retina such as glaucoma [44], a progressive optic neuropathy that affects retinal ganglion cells.

Since long term transgene expression is integral to the success of any gene therapy intervention, we evaluated the expression of the gene 7 and 28 days after the subretinal and intravitreal injections in rat retinas (Figs. 7 and 8, see Supplementary data). 7 days after intravitreal injection, EGFP expression was mainly localized in the ganglion cell layer (GCL), as observed in Fig. 7A. Regarding subretinal injection (Fig. 7B), transfection was mainly observed in the retinal pigment epithelium layer (RPE) 7 days after the injection. Likewise, EGFP was observed in both the outer and inner nuclear layers and in some retinal ganglion cells (RGC) close to the site of injection. At 28 days (Fig. 8), we still found many transfected cells in the RPE after subretinal injection (Fig. 8A, B). Regarding intravitreal injection, transfection efficiency was maintained in the internal layers of the retina 28 days after the injection, as observed in Fig. 8C and D.

These preliminary results offer reasonable hope, since long-term expression is an important handicap that non-viral approaches need to overcome in order to translate retinal gene therapy approaches from animal research into clinical trials [45]. In addition, differences in anatomy, physiology, development and biological phenomena between rats and human should be considered when correlating results of any research where time is a crucial factor. For instance, it has been estimated that one lived day for rats is comparable to 30 lived days for humans [46]. As transgene expression duration depends of many factors, which are related not only with the formulation design, but also with the vector design [1], additional work will be required to address this mandatory issue.

To further determine whether exposure to lipoplexes had any inflation effect on the vitreous after subretinal injection, a more invasive route than intravitreal, we performed an analysis of the eye fundus 28 days after the subretinal injection, since it has been shown that this amount of time is sufficient for full functional recovery from any possible retinal detachment due to injection procedures [47]. As showed in Fig. 8 (Supplementary data), we did not observe any retinal detachment nor signs of retinal pathology in the fundus image of the retina. Therefore, the lack of inflammation in the vitreous along with the positive gene expression profile suggests that our formulation may be an interesting approach for targeting inherited retinal diseases.

5. Conclusions

In this study we have elaborated and characterized a safe and easy way to prepare niosome formulation based on the cationic lipid 2,3-di(tetradecyloxy)propan-1-amine, combined with squalene and

polysorbate 80, to transfect efficiently the retina. Targeted cells strongly depended on the administration route. Whereas subretinal injections transfected mainly the RPE layer; the intravitreal injection transfected a broad surface in the inner layers of the retina. Although this preliminary study offers hope to deliver genetic material to the retina by a safe non-viral vector formulation, additional work would be required to target the outer retina by the much safer intravitreal instead of the subretinal injections, in order to translate preclinical results in animals to real patients.

Supplementary data to this article can be found online at http://dx.doi.org/10.1016/j.jconrel.2013.11.004.

Acknowledgment

This project was partially supported by the University of the Basque Country UPV/EHU (UFI 11/32), by the Basque Goverment (predoctoral BFI-2011-226 grant), by CONACYT, Mexico (Grant Reg. 217101), by the Research Chair in Retinosis Pigmentosas "Bidons Egara" and by Spanish grants MAT2012-39290-C02-01 and IPT-2012-0574-300000. Technical and human support provided by SGIker (UPV/EHU) are gratefully acknowledged.

References

[1] D.M. Lipinski, M. Thake, R.E. MacLaren, Clinical applications of retinal gene therapy, Prog. Retin. Eye Res. 32 (2013) 22–47.
[2] M.E. McClements, R.E. MacLaren, Gene therapy for retinal disease, Transl. Res. 161 (4) (2013) 241–254.
[3] P. Charbel Issa, M. Groppe, R.E. MacLaren, Gene therapy for retinal dystrophies, Ophthalmologe 109 (2) (2012) 121–128.
[4] R. Naik, A. Mukhopadhyay, M. Ganguli, Gene delivery to the retina: focus on non-viral approaches, Drug Discov. Today 14 (5–6) (2009) 306–315.
[5] P. Colella, A. Auricchio, Gene therapy of inherited retinopathies: a long and successful road from viral vectors to patients, Hum. Gene Ther. 23 (8) (2012) 796–807.
[6] J.W. Bainbridge, A.J. Smith, S.S. Barker, S. Robbie, R. Henderson, K. Balaggan, A. Viswanathan, G.E. Holder, A. Stockman, N. Tyler, S. Petersen-Jones, S.S. Bhattacharya, A.J. Thrasher, F.W. Fitzke, B.J. Carter, G.S. Rubin, A.T. Moore, R.R. Ali, Effect of gene therapy on visual function in Leber's congenital amaurosis, N. Engl. J. Med. 358 (21) (2008) 2231–2239.
[7] A.M. Maguire, F. Simonelli, E.A. Pierce, E.N. Pugh Jr., F. Mingozzi, J. Bennicelli, S. Banfi, K.A. Marshall, F. Testa, E.M. Surace, S. Rossi, A. Lyubarsky, V.R. Arruda, B. Konkle, E. Stone, J. Sun, J. Jacobs, L. Dell'Osso, R. Hertle, J.X. Ma, T.M. Redmond, X. Zhu, B. Hauck, O. Zelenaia, K.S. Shindler, M.G. Maguire, J.F. Wright, N.J. Volpe, J.W. McDonnell, A. Auricchio, K.A. High, J. Bennett, Safety and efficacy of gene transfer for Leber's congenital amaurosis, N. Engl. J. Med. 358 (21) (2008) 2240–2248.
[8] N. Provost, G. Le Meur, M. Weber, A. Mendes-Madeira, G. Podevin, Y. Cherel, M.A. Colle, J.Y. Deschamps, P. Moullier, F. Rolling, Biodistribution of rAAV vectors following intraocular administration: evidence for the presence and persistence of vector DNA in the optic nerve and in the brain, Mol. Ther. 11 (2) (2005) 275–283.
[9] G. Puras, J. Zarate, A.R. Diaz, M. Aviles-Triguero, E. Fernandez, J.L. Pedraz, Oligochitosan polyplexes as carriers for retinal gene delivery, Eur. J. Pharm. Sci. 48 (2013) 323–335.
[10] G. Puras, J. Zarate, M. Aceves, A. Murua, A.R. Diaz, M. Aviles-Triguero, E. Fernandez, J.L. Pedraz, Low molecular weight oligochitosans for non-viral retinal gene therapy, Eur. J. Pharm. Biopharm. 83 (2013) 131–140.
[11] R. Farjo, J. Skaggs, A.B. Quiambao, M.J. Cooper, M.I. Naash, Efficient non-viral ocular gene transfer with compacted DNA nanoparticles, PLoS One 1 (2006) e38.
[12] S. Kawakami, A. Harada, K. Sakanaka, K. Nishida, J. Nakamura, T. Sakaeda, N. Ichikawa, M. Nakashima, H. Sasaki, In vivo gene transfection via intravitreal injection of cationic liposome/plasmid DNA complexes in rabbits, Int. J. Pharm. 278 (2) (2004) 255–262.
[13] Y. Zhang, F. Schlachetzki, J.Y. Li, R.J. Boado, W.M. Pardridge, Organ-specific gene expression in the rhesus monkey eye following intravenous non-viral gene transfer, Mol. Vis. 9 (2003) 465–472.
[14] R. Rajera, K. Nagpal, S.K. Singh, D.N. Mishra, Niosomes: a controlled and novel drug delivery system, Biol. Pharm. Bull. 34 (7) (2011) 945–953.
[15] S. Grijalvo, S.M. Ocampo, J.C. Perales, R. Eritja, Synthesis of lipid–oligonucleotide conjugates for RNA interference studies, Chem. Biodivers. 8 (2) (2011) 287–299.
[16] P. Couvreur, "Squalenoylation": a new approach to the design of anticancer and antiviral nanomedicines, Bull. Acad. Natl Med. 193 (3) (2009) 663–673(discussion 673-664).
[17] L.H. Reddy, P. Couvreur, Squalene: a natural triterpene for use in disease management and therapy, Adv. Drug Deliv. Rev. 61 (15) (2009) 1412–1426.
[18] Y.J. Kim, T.W. Kim, H. Chung, I.C. Kwon, H.C. Sung, S.Y. Jeong, The effects of serum on the stability and the transfection activity of the cationic lipid emulsion with various oils, Int. J. Pharm. 252 (1–2) (2003) 241–252.
[19] F. Liu, J. Yang, L. Huang, D. Liu, Effect of non-ionic surfactants on the formation of DNA/emulsion complexes and emulsion-mediated gene transfer, Pharm. Res. 13 (11) (1996) 1642–1646.
[20] O. Meyer, D. Kirpotin, K. Hong, B. Sternberg, J.W. Park, M.C. Woodle, D. Papahadjopoulos, Cationic liposomes coated with polyethylene glycol as carriers for oligonucleotides, J. Biol. Chem. 273 (25) (1998) 15621–15627.
[21] G. Kokotos, R. Verger, A. Chiou, Synthesis of 2-Oxo amide triacylglycerol analogues and study of their inhibition effect on pancreatic and gastric lipases, Chemistry 6 (22) (2000) 4211–4217.
[22] A.M. Aberle, F. Tablin, J. Zhu, N.J. Walker, D.C. Gruenert, M.H. Nantz, A novel tetraester construct that reduces cationic lipid-associated cytotoxicity. Implications for the onset of cytotoxicity, Biochemistry 37 (18) (1998) 6533–6540.
[23] A. del Pozo-Rodriguez, D. Delgado, M.A. Solinis, A.R. Gascon, J.L. Pedraz, Solid lipid nanoparticles: formulation factors affecting cell transfection capacity, Int. J. Pharm. 339 (1–2) (2007) 261–268.
[24] W. Ding, T. Izumisawa, Y. Hattori, X. Qi, D. Kitamoto, Y. Maitani, Non-ionic surfactant modified cationic liposomes mediated gene transfection *in vitro* and in the mouse lung, Biol. Pharm. Bull. 32 (2) (2009) 311–315.
[25] O. Paecharoenchai, N. Niyomtham, T. Ngawhirunpat, T. Rojanarata, B.E. Yingyongnarongkul, P. Opanasopit, Cationic niosomes composed of spermine-based cationic lipids mediate high gene transfection efficiency, J. Drug Target. 20 (9) (2012) 783–792.
[26] S. Resina, P. Prevot, A.R. Thierry, Physico-chemical characteristics of lipoplexes influence cell uptake mechanisms and transfection efficacy, PLoS One 4 (6) (2009) e6058.
[27] R.A. Bejjani, D. BenEzra, H. Cohen, J. Rieger, C. Andrieu, J.C. Jeanny, G. Gollomb, F.F. Behar-Cohen, Nanoparticles for gene delivery to retinal pigment epithelial cells, Mol. Vis. 11 (2005) 124–132.
[28] S. Kachi, Y. Oshima, N. Esumi, M. Kachi, B. Rogers, D.J. Zack, P.A. Campochiaro, Nonviral ocular gene transfer, Gene Ther. 12 (10) (2005) 843–851.
[29] L. Peeters, N.N. Sanders, K. Braeckmans, K. Boussery, J. Van de Voorde, S.C. De Smedt, J. Demeester, Vitreous: a barrier to nonviral ocular gene therapy, Invest. Ophthalmol. Vis. Sci. 46 (10) (2005) 3553–3561.
[30] A. del Pozo-Rodriguez, S. Pujals, D. Delgado, M.A. Solinis, A.R. Gascon, E. Giralt, J.L. Pedraz, A proline-rich peptide improves cell transfection of solid lipid nanoparticle-based non-viral vectors, J. Control. Release 133 (1) (2009) 52–59.
[31] S. Xiang, H. Tong, Q. Shi, J.C. Fernandes, T. Jin, K. Dai, X. Zhang, Uptake mechanisms of non-viral gene delivery, J. Control. Release 158 (3) (2012) 371–378.
[32] J. Rejman, A. Bragonzi, M. Conese, Role of clathrin- and caveolae-mediated endocytosis in gene transfer mediated by lipo- and polyplexes, Mol. Ther. 12 (3) (2005) 468–474.
[33] A. Ferrari, V. Pellegrini, C. Arcangeli, A. Fittipaldi, M. Giacca, F. Beltram, Caveolae-mediated internalization of extracellular HIV-1 tat fusion proteins visualized in real time, Mol. Ther. 8 (2) (2003) 284–294.
[34] D. Delgado, A. Del Pozo-Rodriguez, M.A. Solinis, A.R. Gascon, Understanding the mechanism of protamine in solid lipid nanoparticle-based lipofection: the importance of the entry pathway, Eur. J. Pharm. Biopharm. 79 (3) (2011) 495–502.
[35] I.A. Khalil, K. Kogure, H. Akita, H. Harashima, Uptake pathways and subsequent intracellular trafficking in nonviral gene delivery, Pharmacol. Rev. 58 (1) (2006) 32–45.
[36] J. Rejman, M. Conese, D. Hoekstra, Gene transfer by means of lipo- and polyplexes: role of clathrin and caveolae-mediated endocytosis, J. Liposome Res. 16 (3) (2006) 237–247.
[37] J.P. Luzio, M.D. Parkinson, S.R. Gray, N.A. Bright, The delivery of endocytosed cargo to lysosomes, Biochem. Soc. Trans. 37 (Pt 5) (2009) 1019–1021.
[38] A.K. Varkouhi, M. Scholte, G. Storm, H.J. Haisma, Endosomal escape pathways for delivery of biologicals, J. Control. Release 151 (3) (2011) 220–228.
[39] I.S. Zuhorn, U. Bakowsky, E. Polushkin, W.H. Visser, M.C. Stuart, J.B. Engberts, D. Hoekstra, Nonbilayer phase of lipoplex–membrane mixture determines endosomal escape of genetic cargo and transfection efficiency, Mol. Ther. 11 (5) (2005) 801–810.
[40] V. Allain, C. Bourgaux, P. Couvreur, Self-assembled nucleolipids: from supramolecular structure to soft nucleic acid and drug delivery devices, Nucleic Acids Res. 40 (5) (2012) 1891–1903.
[41] S.M. Conley, M.I. Naash, Nanoparticles for retinal gene therapy, Prog. Retin. Eye. Res. 29 (5) (2010) 376–397.
[42] M.M. Hims, S.P. Diager, C.F. Inglehearn, Retinitis pigmentosa: genes, proteins and prospects, Dev. Ophthalmol. 37 (2003) 109–125.
[43] P. Dureau, L. Legat, M. Neuner-Jehle, S. Bonnel, S. Pecqueur, M. Abitbol, J.L. Dufier, Quantitative analysis of subretinal injections in the rat, Graefes Arch. Clin. Exp. Ophthalmol. 238 (7) (2000) 608–614.
[44] X. Liu, C.A. Rasmussen, B.T. Gabelt, C.R. Brandt, P.L. Kaufman, Gene therapy targeting glaucoma: where are we? Surv. Ophthalmol. 54 (4) (2009) 472–486.
[45] P. Charbel Issa, R.E. MacLaren, Non-viral retinal gene therapy: a review, Clin. Experiment. Ophthalmol. 40 (1) (2012) 39–47.
[46] N.A. Andreollo, E.F. Santos, M.R. Araujo, L.R. Lopes, Rat's age versus human's age: what is the relationship? Arq. Bras. Circ. Dig. 25 (1) (2012) 49–51.
[47] A. Koirala, R.S. Makkia, M.J. Cooper, M.I. Naash, Nanoparticle-mediated gene transfer specific to retinal pigment epithelial cells, Biomaterials 32 (35) (2011) 9483–9493.